Netherlands Journal of Geosciences — Geologie en Mijnbouw | 91 – 3 | 325 - 339 | 2012

Morphodynamics of a storm-dominated, shallow tidal inlet: the Slufter, the Netherlands

M. van der Vegt* **& P. Hoekstra**

Institute for Marine and Atmospheric Research Utrecht, Department of Physical Geography, Utrecht University, P.O. Box 80125, 3508 TC Utrecht, the Netherlands

* Corresponding author. Email: m.vandervegt@uu.nl.

Manuscript received: July 2011, accepted: September 2012

Abstract

In this article we study the morphodynamics of the Slufter on the short-term (months) and long-term (years to decades). The Slufter is a small, shallow tidal inlet located on the island of Texel, the Netherlands. A narrow (tens of meters) channel connects the North Sea with a dune valley of 400 ha. This narrow channel is located in between a 400-700 m wide opening in the dunes. Approximately 80% of the basin of the Slufter is located above mean high water level and is flooded only during storms, when a threshold water level is exceeded.

Analysis of historical aerial photographs revealed that the inlet channel migrates about 100 m per year. In the 1970's it migrated to the south, while since 1980 it is migrating to the north. When the channel reached the dunes at the north side of the dune breach the channel was relocated to the south by man. The channel inside the backbarrier basin was less dynamic. It shows a gradual growth and southward migration of a meander on a decadal time scale.

The short-term dynamics of the Slufter were studied during a field campaign in 2008. The campaign aimed at identifying the dominant hydrodynamic processes and morphological change during fair weather conditions and during storm events. During fair weather flow velocities in the main inlet channel were 0.5-0.8 m/s at water depths of 0-1.5 m, slightly ebb-dominant and associated morphological change was small. When water levels were above critical levels during a storm period the hydrodynamics in the main channel drastically changed. The flow in the main channel was highly ebb dominant. Long ebb periods with typical flow velocities of 2 m/s were alternated by much shorter flood periods with typical velocities of 0.5-1 m/s. This resulted in a net outflow of water via the main channel, while we measured a net inflow of water at the beach plain. During the storm period in 2008 we measured a 10 m migration of the channel to the north.

We conclude that the Slufter is a storm-dominated tidal inlet system.

Keywords: Storm-dominated tidal inlets, Slufter, Wadden Sea, shallow water, beach plain, morphological evolution, field measurements.

Introduction

The aim of this paper is to describe and understand the short-term (weeks to months) and long-term (years to decades) morphodynamic evolution of the Slufter: a secondary tidal inlet system located on the barrier island of Texel, the Netherlands.

Along many sandy coastlines chains of barrier islands are found, intersected by tidal inlets (e.g., Hubbard et al., 1979; Ehlers, 1998; FitzGerald, 1996). We will call these primary tidal inlet systems throughout this paper. Typical examples of these systems can be found along the Dutch and German Wadden coast (Ehlers, 1988), along the east coast of the USA (Hubbard et al., 1979; Davis & Hayes, 1984) and Adriatic coast of Italy. The morphodynamics of these systems have been studied extensively (for a review see de Swart & Zimmerman (2009)) and many empirical relationships have been identified (eg., O'brien, 1969; Walton & Adams, 1976; Eysink, 1990; Powell et al., 2006).

Secondary tidal inlet systems (called slufters in Dutch) are present along breached sand bank systems or along dunes with a low-lying former beach plain that can serve as the back-barrier basin(van Bohemen, 1996). A small channel connects the basin with the sea. The breached sand bank systems are in general

https://doi.org/10.1017/S0016774600000470 Published online by Cambridge University Press

short-lived (maximum years), while breaches in the fore dune can survive for decades or longer. The main differences between primary and secondary tidal inlet systems are the typical length and width of the basin (hundreds of meters vs kilometres), the typical depth of the inlet (few meters vs. tens of meters) and the tidal prism (10^5-10^6 m^3 vs 10^7-10^8 m^3). Furthermore, the bed-level in the backbarrier basin and in the inlet is relatively high, resulting in large differences in wetted basin area between fair weather and storm conditions and truncation of the tidal signal (Lincoln & FitzGerald, 1988). These differences between primary and secondary tidal inlet systems must have strong implications for their morphodynamic evolution. The size and forcing of secondary inlets are closely related to those of ephemeral inlets (or intermittently open/closed inlets (Cooper, 2001) and washover systems (Donnely et al., 2006).

The Slufter is a typical example of a secondary inlet (van der Vegt et al, 2009) and is shown in Fig. 1. The photo shows the Slufter looking to the north. Only a small part of the basin was flooded at the moment of the photo, which was taken during fair weather conditions. The picture also shows the primary tidal inlet Eyerlandsche gat, which is the tidal inlet between Texel and Vlieland (the first two barrier isands, see inset of Fig. 1). The differences in scale and setting (primary tidal inlet is located between two barrier islands, secondary inlet is on the barrier island) can be seen from this photo. Other examples of secondary tidal inlets are Het Zwin at the Dutch-Belgium borders and the Zwarte Polder at the south-west delta of the Netherlands (van Bohemen, 1996), de Kerf (Meerkerk, 2007).

Due to the local gradients in salinity, water content of the sediment, sediment composition and nutrient availability, unique plant species can survive and secondary inlets have large ecological value (Bowman, 1993; Meerkerk et al., 2007). To develop nature, secondary tidal inlets are sometimes artificially created by for instance breaching dunes. These secondary tidal inlet systems are often designed by down-scaling the rule-based knowledge obtained from primary tidal inlets. This often results in wrong design of such tidal inlet systems and several attempts to create secondary tidal inlets have failed (Bowman, 1993; Meerkerk et al., 2007).

In this article we try to identify the key processes and parameters that are determinative for the hydro- and morphodynamics of secondary inlets by studying the dynamics of the Slufter. Our main objective is to discuss and study its dynamics on both the long-term (years) and short term (weeks). Based on historical data we describe the long-term morphological evolution of the Slufter, and using the results of a six week field campaign we will indentify the key hydrodynamic processes for its evolution on the time scale of weeks to months. In the discussion we will compare the dynamics of secondary tidal inlets with those of salt marshes, washover areas and primary tidal inlets.

Physical setting

The Slufter is located on the island of Texel, the Netherlands. Texel is the most southern island of the Wadden islands. This chain of barrier islands stretches out from the Netherlands, along the German coast to Denmark (see inset Fig. 1 for the Dutch part). The length of the barrier islands and size of the tidal inlet systems gradually decreases from Texel to the German Bight, after which it increases again (van der Vegt et al., 2007; Oost & de Boer, 1994). The tides are semi-diurnal and the average tidal range increases from 1.7 m near Texel to a maximum of 3 m near the German Bight, after which it decreases again. Largest

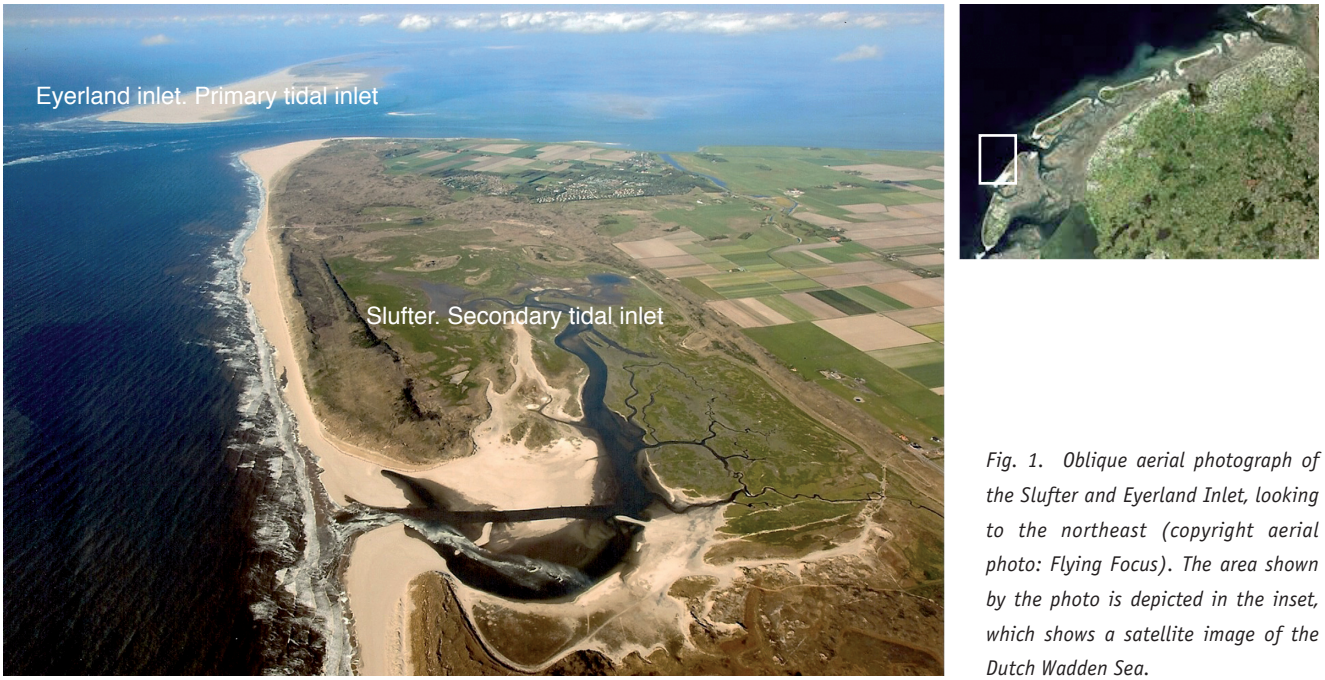

Fig. 1. Oblique aerial photograph of the Slufter and Eyerland Inlet, looking to the northeast (copyright aerial photo: Flying Focus). The area shown by the photo is depicted in the inset, which shows a satellite image of the Dutch Wadden Sea.

https://doi.org/10.1017/S0016774600000470 Published online by Cambridge University Press

waves are from the west and north-west and significant wave height is approximately constant along the Wadden islands (Sha, 1989).

Texel is the first and largest of the Wadden islands. Typical tidal range at the North Sea at neap tide is 1.4 m and is 2.1 m at spring tide. The tides are mainly semidiurnal, but have a clear diurnal inequality. Wave statistics from the measuring pole of the Eyerlandse Gat (4.662 degrees North, 53.277 degrees East) reveal that for Texel the long-term mean significant wave height is 1.4 m and significant period is 5.8 s. Waves come from directions between south and north, with a dominantly westerly component. Most energetic waves are from the north and northwest due to longer wind fetch at the North Sea for these conditions.

The Slufter on Texel is located at the position of a former tidal inlet that separated the barrier island Eyerland from Texel. During the 16th and 17th century this inlet was largely silted up. Human intervention (reclaiming of land) resulted in a connection of the two barrier islands. To prevent flooding of the reclaimed land, in 1630 a 6 km long sand drift dyke was constructed approximately 1.5 km landward of the coastline. This sand drift dyke still exists and is nowadays the eastern border of the Slufter basin. In 1855 another sand drift dyke was constructed parallel to the older one, but located 1.5 km to the west. In 1858 this westerly sand drift dyke was breached at three positions. Two breaches were closed by man, but the third one remained open. This breach evolved and has become what is now called the Slufter. The opening in the dunes is nowadays 400 m wide, but used to be 700 m till the 1960's. The main channel of the Slufter is about 30 m wide and intersects the beach plain between the two dune rows. Large parts of the beach plain are supratidal and are only flooded when critical levels are exceeded.

Research Approach

Morphological reconstruction: Aerial photographs and coastal profiles

We have aerial, orthogonal photographs of the seaward side of the Slufter for the years 1954 and 1975 till 1997 (almost every year). These photos are used to qualitatively reconstruct the morphological evolution of the main inlet channel. For most photographs the height of the flight was recorded and the focal length is known. Based on this the scale of the photo was determined.

Since 1963 cross-shore transects of the bed level of the Dutch coastal zone are measured from approximately 5 m depth till the dunes. These transects are measured each year and have an alongshore spacing of 200 m. All transects have a fixed orientation with respect to the north (approximately shore-normal) and start at a fixed reference point (beach pole). This JARKUS dataset is maintained and provided by Rijkswaterstaat, presently part of the Dutch ministry of Infrastructure and the Environment (hereafter data from this source is referred to as RWS). The JARKUS data are ideal to show the general eroding or accreting trends along the Slufter on Texel.

Process based field observations

A field campaign was performed in the autumn of 2008. It was aimed at identifying the dominant physical processes and morphological change in the Slufter during calm weather and storm conditions. An overview of the measurement locations is shown in Fig. 2. Detailed information about sensor types, sensor heights, measurement protocols and measurement period for the different locations is provided in Table 1. One measurement rig was located in the main channel during the entire fieldwork. The main aim was to identify the water levels, waves and flow velocities at the entrance channel. Because the main channel migrated due to an erosion deposition sequence the frame was shifted 20 m to the north at Julian day 280. Water levels were measured continuously at 4 Hz at 15 cm above the bed (from

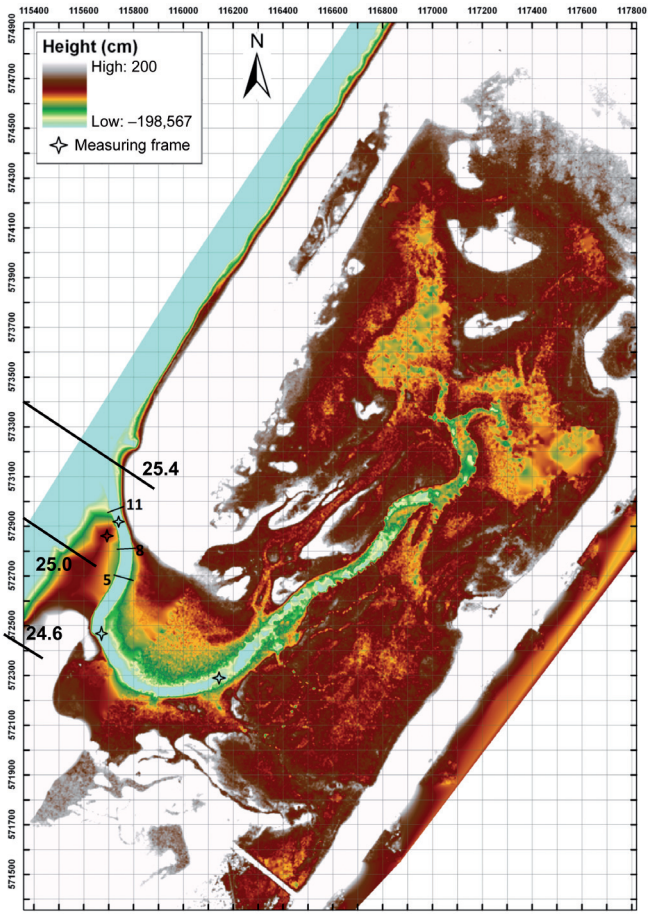

Fig. 2. Color plot of the bathymetry of Slufter mouth area and backbarrier basin. The total area shown is 2.4 by 3.5 km and each cell represents 100 by 100 m. Profiles 5, 8 and 11 are three of the 13 cross-channel profiles that were monitored during the field campaign. Profiles 24.6, 25.0 and 25.4 are the profiles that measured on a yearly base (JARKUS data).

https://doi.org/10.1017/S0016774600000470 Published online by Cambridge University Press

Table 1. Overview of measurement locations and parameters that were measured. EMF means electromagnetic flowmeter.

Main frame					
Where	What	Sensor	Level (m)	Period (day in 2008)	Protocol
Inlet channel	Flow velocity	EMF	−0.35	262-300	4 Hz continuous
		EMF	−0.25	262-300	4 Hz continuous
		EMF	+0.15	262-300	4 Hz continuous
	Water level	Pressure	−0.35	262-300	4 Hz continuous
Mobile frame					
Where	What	Sensor	Level (m)	Period (day in 2008)	Protocol
Meander bend	Flow velocity	EMF	−0.30	264-267	2 hz continuous
				268-271	Burst mode: 4 Hz, 17 min per 30 min
	Water level	Pressure	−0.25	264-267	2 hz continuous
				268-271	Burst mode: 4 Hz, 17 min per 30 min
Upstream	Flow velocity	EMF	−0.53	264-267	2 hz continuous
				268-271	Burst mode: 4 Hz, 17 min per 30 min
	Water level	Pressure	−0.53	264-267	2 hz continuous
				268-271	Burst mode: 4 Hz, 17 min per 30 min
Beach plain	Flow velocity	EMF	+1.15	274-277	Burst mode: 4 Hz, 17 min per 30 min
	Water level	Pressure	+1.10	274-277	Burst mode: 4 Hz, 17 min per 30 min

here on: cmab) using a Keller pressure sensor. The pressure was corrected for air pressure by using an automatic weather station. Flow velocities were measured continuously at 4 Hz at 15 cm and 25 cm above the bed (cmab) using two electromagnetic flow meters (EMF).

Also two mobile frames were deployed in the field. They were equipped with a Keller pressure sensor at 10 cmab and an EMF at 15 cmab. They either sampled at 4 Hz for 17 minutes each half an hour or measured continuously at 2Hz. During calm weather the mobile frames were located inside the backbarrier basin, to characterise the filling and emptying of the shallow basin. During storm the two mobiles frames were located on the beachplain, to characterise the flow patterns at the beach plain during storm. They were located close to the measurement rig of the main channel. Although only located at a distance of less than 100 m from the rig in the main channel, the difference in bed level was large. Unfortunately, only one of the two frames measured properly during the storm period.

Data was checked for quality. Measurements were identified as spikes when they deviated from the ten minute mean more than three times the standard deviation (Less than 0.1% of the data met this criterion). Missing data and spikes were linearly interpolated to get a full record at 4 Hz if in a ten minute record less than 0.1% of data was classified as a spike. Otherwise data was disregarded.

The morphology of the mouth areas was monitored using a DGPS device. Thirteen transects were defined across the seaward end of the Slufter channel. The transects that are discussed in this paper are shown in Fig. 2. They were surveyed at least at the start and at the end of the field campaign. When morphological change was visible, the transects were also measured.

Determination of tidal prism, cross-sectional area and wetted basin area

Many gross-bathymetrical features of primary tidal inlets scale with the tidal prism. It is defined as the amount of water that flows in and out of the tidal inlet during one tidal period. The tidal prism influences the cross-sectional area (O'Brien, 1969), the stability of the main inlet channel (Bruun & Gerritsen 1960), and is also supposed to determine the intertidal flat area (Eysink, 1990). From the cross-sectionally averaged flow velocities in the inlet and the cross-sectional area (denoted as A_c from here on) the tidal prism can be calculated. However, often only single point measurements are taken and these have to be extrapolated to a cross-sectional mean. Therefore, other techniques have been developed to determine the tidal prism. From detailed maps of the tidal basin the wetted area of the backbarrier basin as a function of water level can be determined, assuming that water levels are uniform within the basin. The tidal prism is then

$$TP = \int_{Z_{min}}^{Z_{max}} A_{xy}(z)dz$$

where Z_{max} is the maximum water level within a tidal period, Z_{min} the minimum water level within a tidal period and A_{xy} is the wetted basin area. In the case that wetted basin area at low and high water are similar (hence tidal flat area is small), the tidal prism equals the basin area times the tidal range. However, for the Slufter the wetted area at low water is considerably smaller than it is at high water and the assumption of constant basin area leads to erroneous estimates of the tidal prism.

We have determined the wetted basin (A_{xy}) area as a function of water level using a digital elevation model of the Slufter

https://doi.org/10.1017/S0016774600000470 Published online by Cambridge University Press

area. For the backbarrier basin this DEM is based on the AHN LIDAR database, which has a resolution of 2-3 m in the horizontal direction and 10 cm in the vertical. Since the mouth area is very dynamic the 2008 bathymetry is different from the 2005 bathymetry. The DEM of the mouth area was therefore based on our own DGPS measurements obtained during the field campaign. The AHN and DGPS dataset were coupled and interpolated based on a natural neighbour method. Using GIS software, the basin area and basin volume as a function of water level were determined assuming that water levels are uniform throughout the basin.

Results

Morphological evolution of the Slufter on the time scale of years to decades

Figure 3 shows the Slufter area in 1954. This photo was taken oblique and from a much larger height than the other photographs. It shows a large part of the Slufter one year after the February 1953 storm, which heavily impacted the coasts along the North Sea. In 1954 the mouth area was very sandy. During the storm the entire inlet was flooded and a washover fan inside the Slufter basin was created. The main channel that drains the backbarrier basin was disconnected, suggesting the Slufter had fallen dry. The whole system might have been closed by the overwash during the February 1953 storm. Furthermore, in 1954 the dune to dune distance at the inlet was large (700 m) compared to the present situation (400 m).

Orthogonal photographs of the Slufter mouth for the years 1975-1979 and 1981 are shown in Fig. 4. In all panels the same area of the Slufter is shown. In 1975 the main channel of the Slufter was oriented shore normal and was positioned just halfway the two dunes. The distance between the dunes had reduced because sand drift dikes were constructed since 1954. In about 4 years time (see photo of 1979) the seaward end of the channel migrated to the south. Inside the basin a small meander in the channel was created, while an old channel had been closed off by man. In 1981 the Slufter channel started migrating to the north.

Figure 5 shows the Slufter mouth area for the years 1992-1995 and 1997. The 1992 photograph shows the mouth area of the Slufter just after the seaward end of the channel had been relocated to the south to protect the northern dunes from erosion. This relocation of the main channel of the Slufter has occurred in 1973, 1983, 1987, 1991, 1998, 2002 and 2009. In 1992 the remnants of the old channel are still visible as dark regions in between the two dune systems. The photographs taken in 1993-1997 show the typical pattern of northward migration of the seaward tip of the channel, followed by channel relocation.

The aerial photographs reveal that the seaward tip of the channel is highly dynamic. In the period 1975-1979 it migrated southward, while since 1980 the trend has reversed and the channel migrates northward. When the channel reaches the dunes it is relocated. The landward part of the channel is less dynamic. It shows a gradual movement to the south and the generation of a large meander. Since 1954 the distance between the northern and southern dunes has been reduced from about 700 m to about 400 m. This was not a natural process but due to the development and extension of artificial sand drift dikes.

To further illustrate the morphological evolution of the Slufter the bed level along several cross-shore transects (JARKUS dataset) is plotted. Figure 6 shows bed level as a function of distance from the transect origin (= beach pole) for 3 transects across the Slufter inlet, for the years 1966, 1976, 1986, 1996 and 2006. Transect 25.0 is located in the centre of the Slufter. Transects 24.6 and 25.4 are located respectively 400 m to the south and north of the central transect. In general, the 1966 bed profiles are located higher than the profiles in later years, indicating net erosion since 1966. This is best illustrated by the 25.0 profile. Since 1979 the beach and shoreface are nourished regularly. In 1995 the Eyerland dam was constructed to reduce sand losses in the northern tip of the island.

Profiles 24.6 and 25.4 reveal the growth in height and width of the dunes since 1966 at the south and north side of the Slufter, respectively. At the south side (24.6) there is a continuous growth in height and width of the dunes. As was shown in the photographs, this was established via sand fences. At the north side (25.4) the dunes also have grown, but this process was less regular. In 1966 there small dunes relatively far seaward, which was then eroded again in 1976. Since 1986 there seems to be a more steady growth of the dunes.

Hydrodynamics

Boundary conditions field campaign

The hydrodynamic boundary conditions for the field campaign (provided by RWS) are shown in Fig. 7. The measured sea surface height with respect to N.A.P. (Dutch ordnance datum) at Texel Noordzee reveals a semidiurnal signal with a daily inequality. There is a clear spring-neap cycle and measured elevations do not deviate much from astronomical tides during. Only from end of September to begin of October (Julian days 274-279) there is a clear set-up of 0.5-1 m, caused by the development and passage of a storm event with winds from the northwest. Because the surge was concurrent with spring tide the entire Slufter basin flooded.

The measured wave parameters (height, peak period and direction) at the Eyerland station show calm weather conditions during large parts of the field campaign (Fig. 8). Nevertheless, several small peak events (significant wave height up to 2 m) and the storm event can be noticed (Julian days 274-279). A more detailed plot of the observed wave parameters (Fig. 9)

https://doi.org/10.1017/S0016774600000470 Published online by Cambridge University Press

Fig. 3. Aerial photograph of the Slufter in 1954, one year after the February 1953 storm that heavily impacted the Dutch coast.

reveals that the storm period is characterised by a sequence of wave events. The maximum wave height rose to 4-5 m and significant wave period was 6-8 s. Wave direction was generally from the west and northwest, while at Julian day 279 waves came in from the southwest. The local coastline is aligned along the line 34-214 degrees north. Shore-normal waves are therefore directed 304 degrees with respect to the north.

Calm weather: Hydrodynamics in the main inlet channel

Figure 10 shows the measured water levels and along-channel flow velocities (at 25 cmab) at the mainframe from Julian day 255 to 272. This was a calm weather period. Spring tide was around day 263 and neap tide around day 270. Note that water levels never fall below –0.5 m, while at the North Sea they drop below –1 m. Large parts of the main channel are above the low water level and the tidal signal in the Slufter is truncated with respect to the signal at the North Sea. In general, the observed high water levels in the slufter are similar to the high water levels at the North Sea (see also Fig. 7). Another interesting feature is the double peak in water levels that are sometimes visible in the water level signal, with the second peak being the largest one. This double peak is also present at the North Sea.

The ten minute averaged flow velocities clearly reveal a double peak in flow velocity during flood, in some cases even separated by a short ebb period (Julian days 261 and 263). The second flood period has smaller flow velocities than the first peak, while water levels are higher during the second peak. Although the low water levels are truncated, the Slufter never fell dry during the measuring period. Ebb is very long (7.5-8 hours) compared to the flood period (4.5-5 hours), but the Slufter keeps on draining water from the backbarrier basin to the sea. However, the last few hours of the ebb period flow velocities become very small and water levels slowly drop. Water levels still drop in the Slufter channel when at the North Sea water levels are increasing again. When water levels in the North Sea reach -0.5 m below N.A.P. also the Slufter starts flooding again. Because the water levels are rising relatively fast at this stage flow velocities increase within one hour from small ebb velocities to peak flood flows. Therefore peak ebb velocities in the main channel of the Slufter occur early in the ebb stage.

Velocity-stage diagrams reveal flow velocities as a function

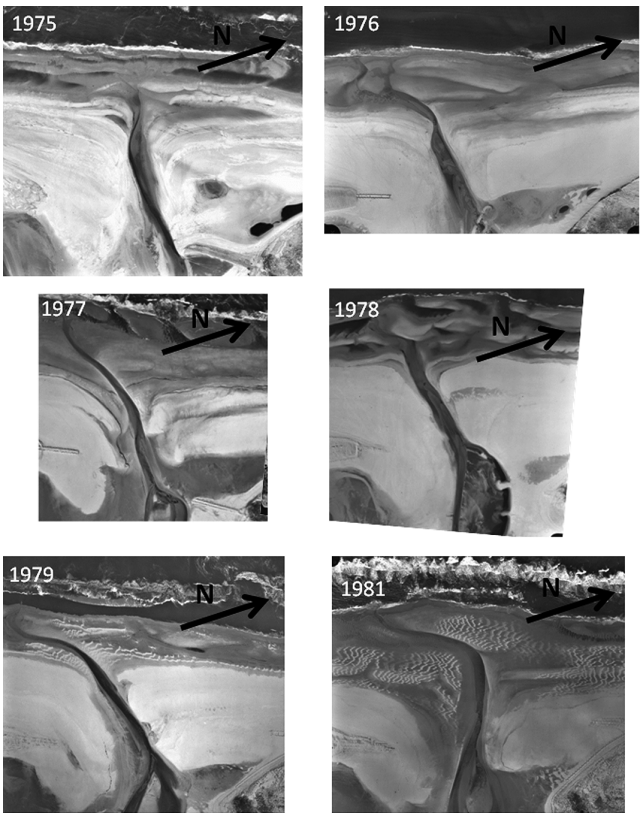

Fig. 4. Orthogonal aerial photographs of the Slufter for the years 1975-1979 and 1981. Photos have been scaled based on height of flight and focal length of the camera.

https://doi.org/10.1017/S0016774600000470 Published online by Cambridge University Press

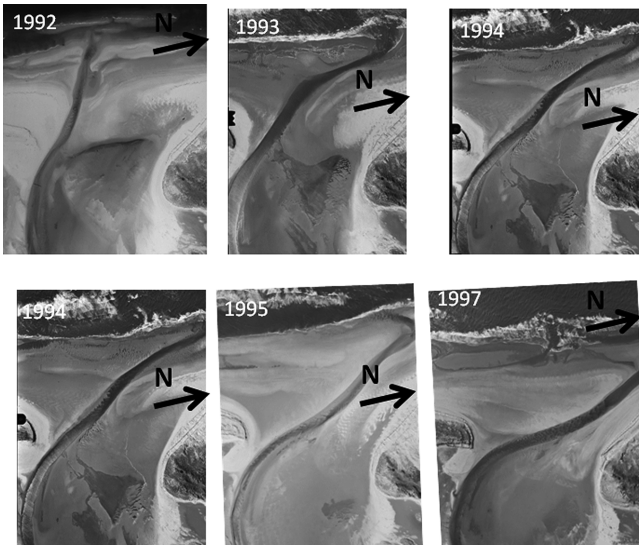

Fig. 5. Orthogonal aerial photographs of the Slufter for the years 1992-1995 and 1997. Photos have been scaled based on height of flight and focal length of the camera.

of water level. Figure 11 shows the results for spring tide/calm weather, neap tide/calm weather and spring tide/storm (discussed in the next paragraph) conditions. At neap tide, maximum water levels are plus 0.5 m and minimum water level is –0.5 m. At high and low water flow velocities are zero, indicating a 90 degrees phase difference between water levels and velocities. Maximum flood velocities occur a little bit before high water, while maximum ebb velocities are around mean water level. The velocity-stage diagram at neap tide is almost symmetric and demonstrates the typical profile of filling and emptying of a channel without intertidal flats (Boon & Byrne, 1981; Blanton et al., 2002).

At spring tide the velocity-stage diagram is asymmetric. Because the low water level is truncated due to the presence of a sill, high water level is significantly larger than the low water level. Maximum flood velocities are reached at 0.75 m, while maximum ebb velocities occur around +0.5 m. Peak ebb velocities are much larger than peak flood velocities.

Calm weather: Hydrodynamics at the upstream location

The two mobile frames were located near the channel bend and after the first channel junction from Julian day 265 till 272. Figure 12 shows water levels and flow velocities measured at the main frame, in the channel bend and further upstream, respectively, for three tidal periods around Julian day 267. The water level and flow velocity data have been averaged over ten minutes. The distance from the main frame to the first channel bend is about 600 m and to the location further upstream 1200 m. Although the total distance between the three measuring stations is small, at ebb and flood pronounced gradients in water level occur. At flood water levels measured at the main frame are higher than at the two upstream locations. However, at high water the gradients in water level are absent. During ebb the most landward location has 10 cm higher water levels than the main frame. The average water levels in the backbarrier are higher than in the inlet. The Slufter only falls dry a few times per year, when strong easterly winds cause an additional set down.

The measured flow velocities reveal that the length of the ebb period increases by half an hour from the inlet to the most

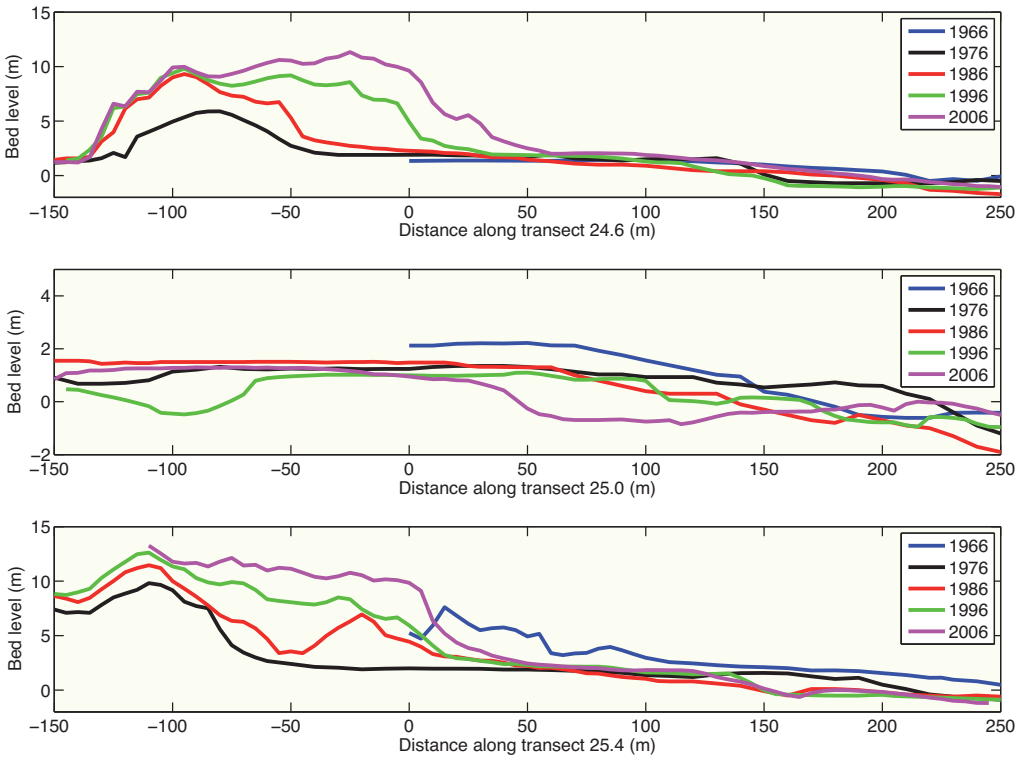

Fig. 6. Bed profiles near Slufter for several years since 1963 based on JARKUS data.

https://doi.org/10.1017/S0016774600000470 Published online by Cambridge University Press

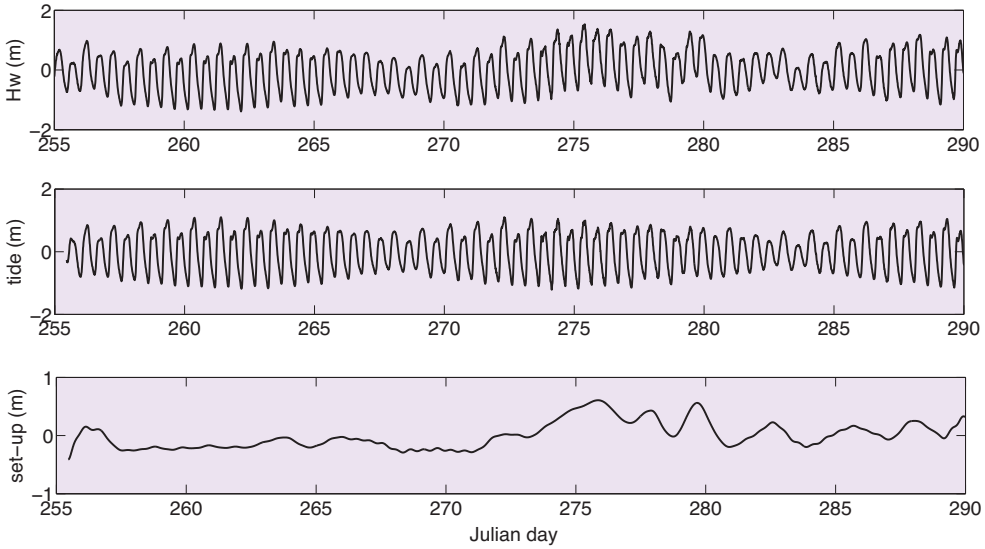

Fig. 7. Measured water levels, predicted astronomical tide and set-up at Texel Noordzee during the field campaign in 2008. Data provided by Rijkswaterstaat.

upstream location. In the most upstream location for almost half an hour the flow is ebbing while water levels rise. Although water levels are rising, locally the sea surface gradient is still directed seaward. The results show that water levels are not homogeneous. Although the Slufter is a small basin, its shallowness causes strong frictional effects, which results in strong deviations from the pumping mode (i.e. uniform water level and phase in tidal basin) that is often considered to be a good approximation of the tidal behaviour of short tidal basins (with respect to the wave length).

Storm conditions: Hydrodynamics in the main inlet channel

The storm period was from Julian day 273-280. The seaward end of the main channel migrated about 10-15 m to the north during this period. Because of this channel migration the main frame, which was originally located in the centre of the 30 m wide channel, got buried under sand. According to the data this occurred at day 276. Hence, we will only analyse the data till day 276. After the storm period the main frame was relocated again to the channel centre. The two mobile frames were located on the beach plain south of the main inlet channel, at about +1 m N.A.P. (see Fig. 2). They were near the main frame, but experienced different conditions due to the difference in water depth.

The hydrodynamics measured at the main frame are shown in Fig. 13. Water levels in the Slufter channel rose to 1.7 m, while at the North Sea maximum water levels were 0.2-0.3 m lower. Probably local wind and wave effects caused additional set-up in the Slufter channel compared to the North Sea station. Water levels at low water were significantly higher in the Slufter than in the North Sea. The ebb period was too short to entirely empty

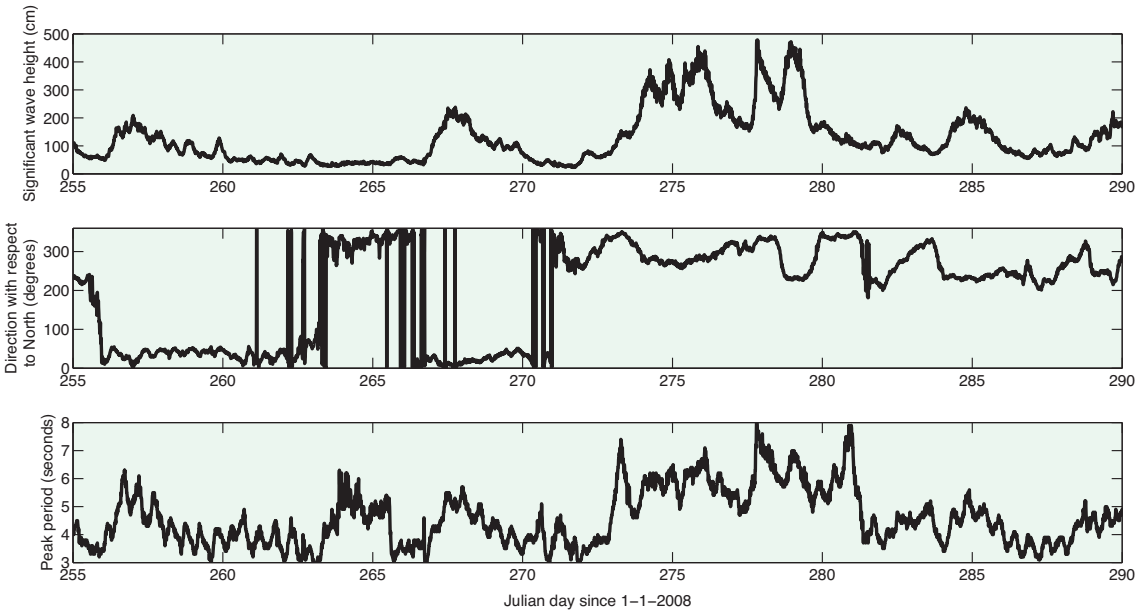

Fig. 8. Wave parameters during field campaign measured at Eyerland.

https://doi.org/10.1017/S0016774600000470 Published online by Cambridge University Press

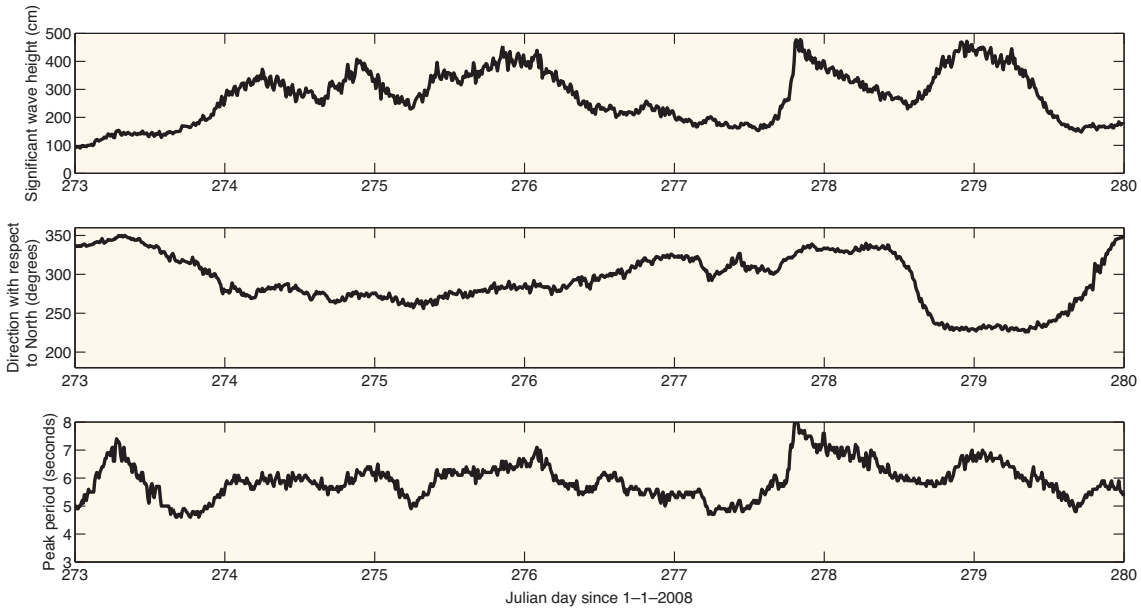

Fig. 9. Measured wave parameters at Eyerland during storm period.

the Slufter basin. Flow velocities during flood were relatively weak compared to the calm weather period. Only at day 274.2 flood flows rose to 1.5 m/s, while for the other displayed data maximum flood velocities were about 0.7 m/s. Though, for large parts of the flood period flow velocities were even much smaller. In contrast, the ebb velocities were very large and 10 minute averaged values peaked at –2 m/s. In addition, the ebb period was longer than the flood period. The sudden change from ebb flows of the order of –1 m/s to flood flows indicate that the ebb period was not long enough to empty the basin. The long period with small ebb velocities that was observed during calm weather periods was absent during the storm period. Probably the cross-sectional area of the inlet was too small at this stage to convey all the water that was present inside the Slufter.

The velocity-stage diagram of the tidal period at day 275 is also depicted in Fig. 11. It is highly asymmetric. Peak flood flows occurred at water levels slightly smaller than +1 m. Flooding of large parts of the tidal basin occurs around +1 m. The maximum water level was above 1.5 m. At high water, flow velocities were still zero, as was the case during calm weather. At low water, however, the main channel was still exporting water at about –1 m/s. Approximately half an hour after low water the channel started flooding. In that period water levels had risen with 30 cm. These results suggest that water levels inside the basin were significantly higher than at sea during the ebb phase. Peak ebb velocities were much larger than peak flood flows and occurred at +0.5 m.

The very long period with strong ebb flows and the relatively short period with weak flood flows resulted in a net export of water through the main channel. Hence, for continuity reasons water should enter the Slufter along different pathways.

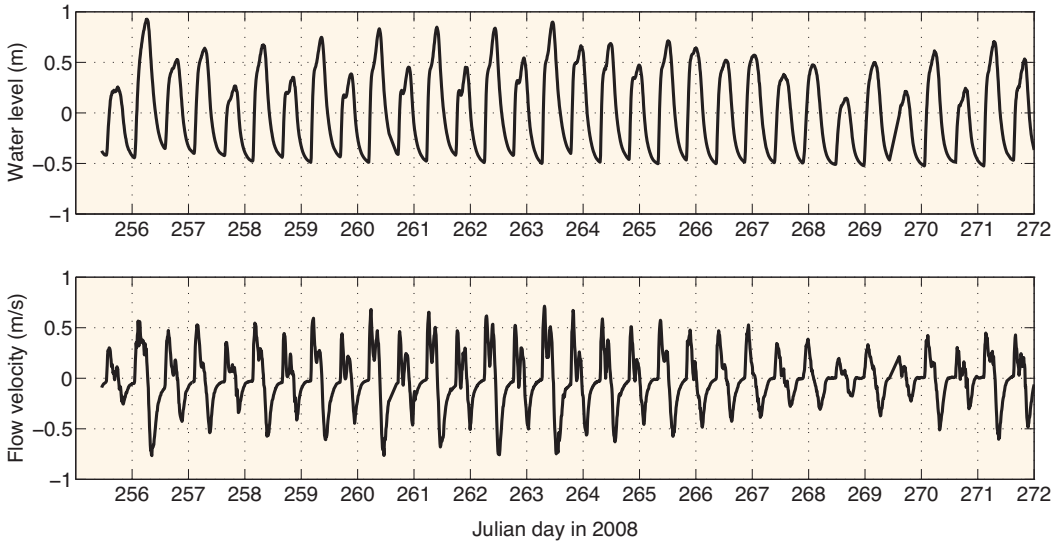

Fig. 10. Hydrodynamics measured by the main frame in the channel during calm weather.

https://doi.org/10.1017/S0016774600000470 Published online by Cambridge University Press

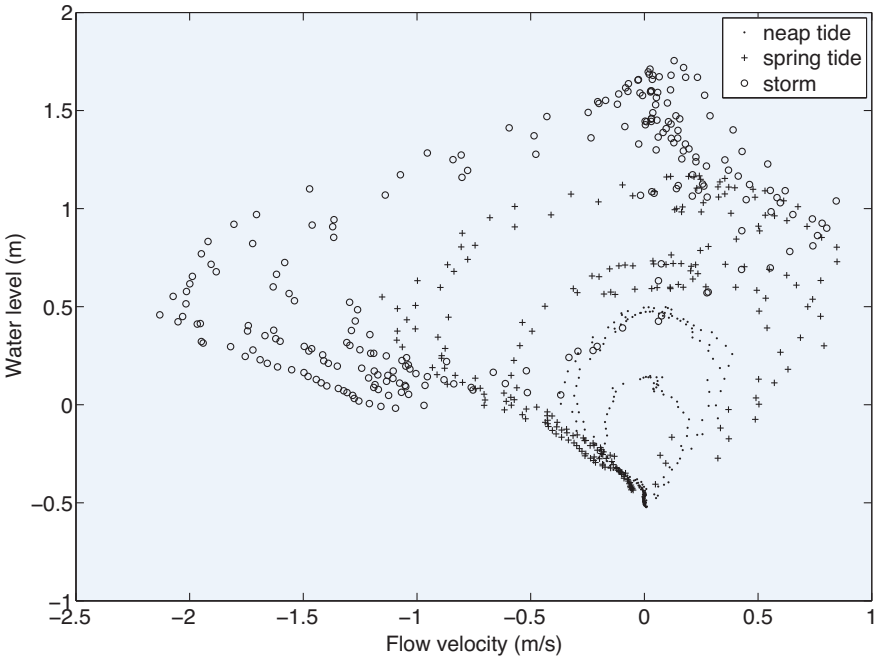

Fig. 11. Velocity-stage diagrams at the main frame during neap tide, spring tide and storm.

Storm conditions: Hydrodynamics at the beach plain

Figure 14 shows the measured water level, cross-shore and along shore flow velocities of the most seaward located mobile frame. Water levels at the beach plain rose to 1.7 meters, which is similar to the water levels at the main frame. Furthermore, because the mobile frame was at a level of +1.0 m, the tide was truncated at this position. We only show results for the case that the frame is submerged with at least 20 cm of water. Measured cross-beach flow velocities reveal that the flood period was longer than the ebb period. Furthermore, the maximum flow velocities at flood were larger than those at ebb. Note that as soon as the beach plain was flooded flow velocities at the main frame were almost zero (compare Fig. 13), while flow velocities at the beach plain were about 0.5 m/s. From that moment the Slufter basin mainly filled by water flowing across the very wide beach plain. During ebb the water left the Slufter basin dominantly via the relatively narrow main channel. Hence, averaged over the tidal period, there is a clear circulation pattern of cross-shore inflow over the beach plain and outflow via the main channel.

Meanwhile, the measured along-shore velocities were directed north. Typical values were 0.2-0.4 m/s. The direction did not change within a tidal period. At Julian days 275 and 276 the direction of waves at the North sea was around 270 degrees (from the west). Because of the orientation of the shoreline near the Slufter (oriented along the line 30-210 degress) this caused the northerly directed along-shore currents.

Wave height reached a maximum of 0.4 m in the channel and on the beach plain (results not shown). We calculated both the wave height for waves with a period till 20 s (wind waves) and waves with a period between 20 and 200 s (infragravity waves). Wind waves and infragravity waves were about equally important, with the infragravity waves being dominant in the early and final stages of flooding, and wind waves at high water.

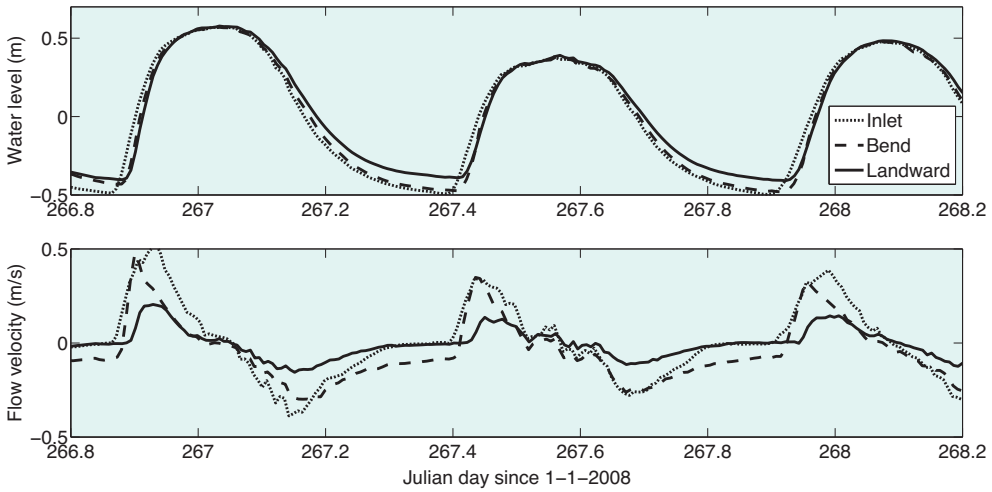

Fig. 12. Hydrodynamics measured inside the backbarrier basin during calm weather period. For location of the measuring stations, see Fig. 2.

https://doi.org/10.1017/S0016774600000470 Published online by Cambridge University Press

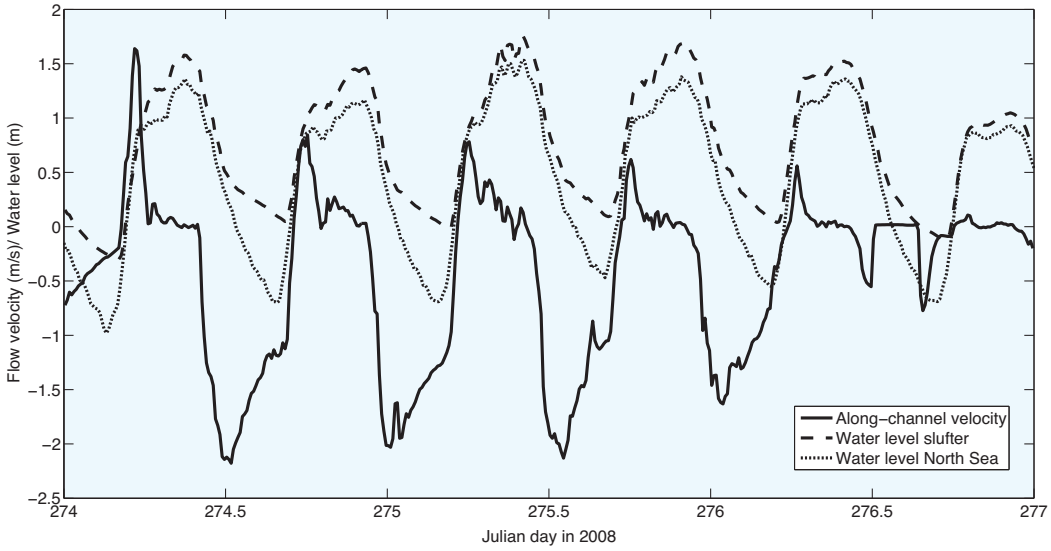

Fig. 13. Hydrodynamics in the main channel during storm period.

Morphological evolution during field campaign

Results of several of the measured cross-channel transects are shown in Fig. 15. The results of transects 5, 8 and 11 show that the channel migrated by eroding its outer bend. The width of the channel increased. The migration of the channel is in the order of 10 m. From visual observations it was clear these morphological changes occurred during the storm period (Julian day 274-280). The results of transects 8 and 11 show that after the storm period the morphological changes were only mall. There was, however, a small decrease in channel width at cross-sections 8 and 11 after the storm period.

Hypsometry of the slufter

Figure 16 shows the wetted basin area, basin volume and wetted cross-sectional area of the inlet as a function of water level for the Slufter. Because water levels never drop below –0.5 m and LIDAR measurements below the mean water level turned out to be less accurate, results are only shown for values above the mean water level. The results clearly reveal the change in basin dimensions above a water level of +1 m N.A.P. Above this level wetted basin area and basin volume strongly. Furthermore, above 1 m the beach plain is also flooded and thereby the cross-sectional area of the inlet strongly increases. The results show that the tidal prism that enters the Slufter strongly depends on the maximum water level reached during a tidal cycle.

The maximum water levels are determined by the astronomical tide, the meteorological tide and wave driven set-up. At the North Sea the tidal range varies between 1.4 m at neap and 2.2 m at spring tide. This results in maximum water levels between 0.7 m and 1.1 m. The meteorological tide, mainly caused by wind, can cause an increase of 2 meters on top of the astronomical tide. Waves also can cause an increase in water levels, but this set-up is small (up to 0.2-0.3 m) with respect to the wind-driven component. However, it is often spatially non-uniform along the coast or within the tidal basin and might influence the flow patterns.

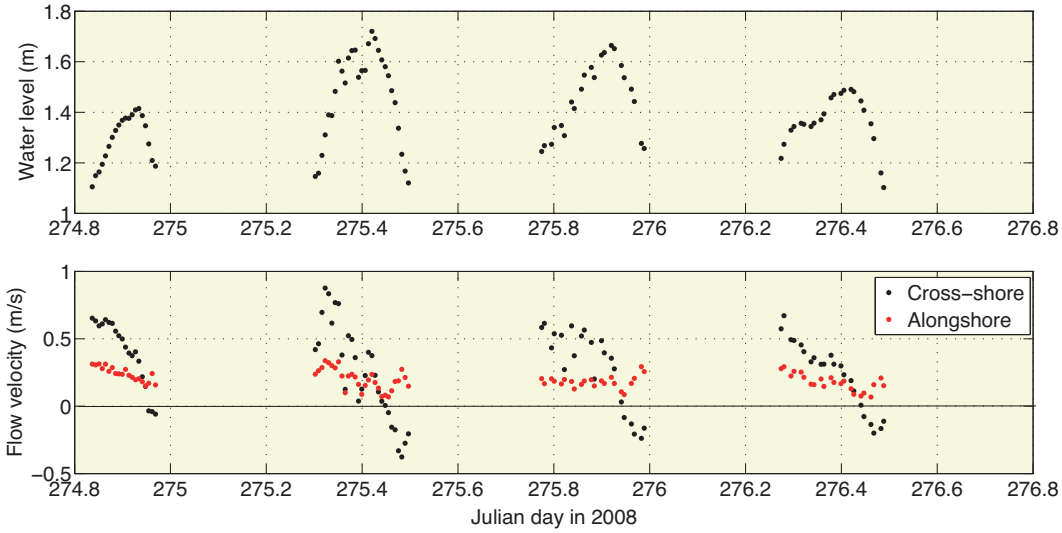

Fig. 14. Hydrodynamics on the beach plain during storm period. For location of measurement location, see Fig. 2.

https://doi.org/10.1017/S0016774600000470 Published online by Cambridge University Press

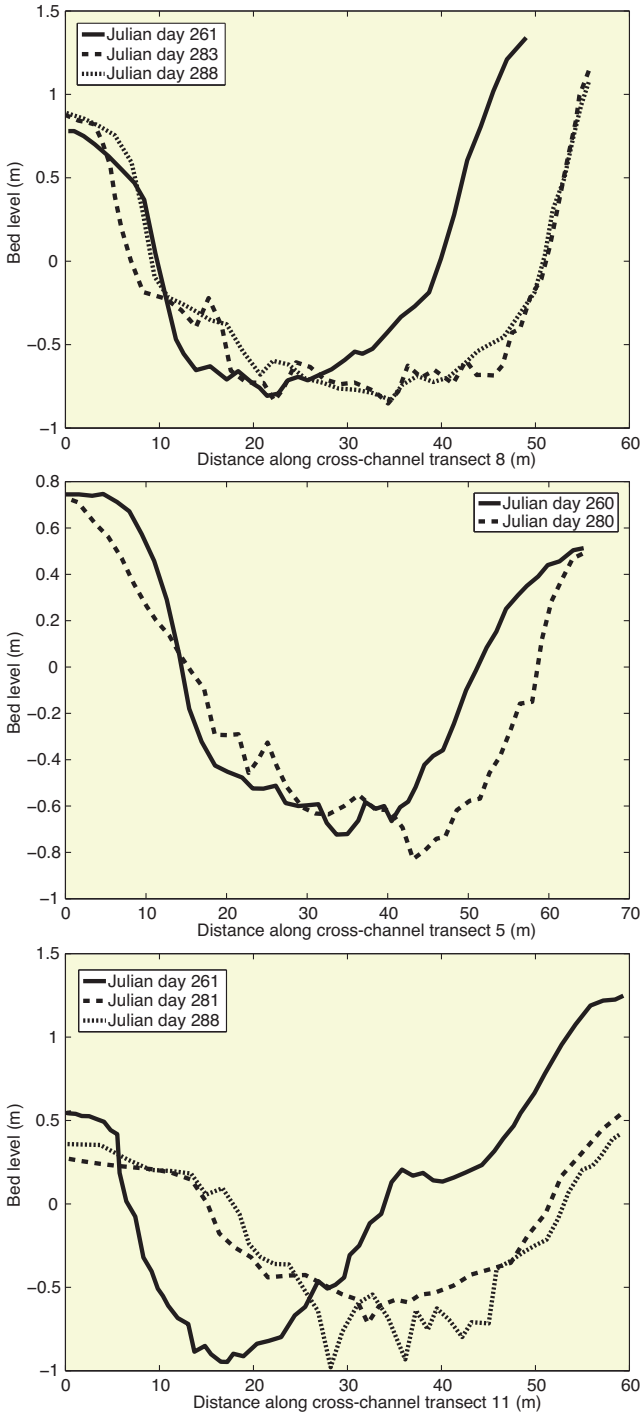

Fig. 15. Measured evolution of cross-channel profiles 5, 8 and 11 during field campaign.

Under fair weather spring tide conditions the maximum water level was approximately +1 m N.A.P. and only the Slufter channel was flooded. This channel is approximately three kilometres long and 50-100 meters wide. The total flooded area at +1 meter amounts to $8{\cdot}10^5$ m^2 and basin volume is $5.7{\cdot}10^5$ m^3. The cross-sectional area of the inlet channel at +1 m N.A.P. is 60 m^2. The average water depth in the Slufter at high water, calculated as the ratio of basin volume and wetted basin area, is approximately 0.7 m.

During the storm period water levels reached 1.6 m. This increase of only 0.6 m compared to the maximum values obtained during fair weather conditions resulted in a wetted basin area at high water of $3.2{\cdot}10^6$ m^2 and basin volume of $1.8{\cdot}10^6$ m^3. This is a three to fourfold increase compared to the fair weather spring tide conditions. The cross-sectional area at +1.6 m is 2600 m^2. The average water depth in the Slufter at high water during the storm period was approximately 0.5-0.6 m. This very small water depth was caused by the large marsh areas in the Slufter that were flooded and only contained very shallow layers of water.

Discussion

The dynamics of secondary tidal inlets compared to primary tidal inlets

The dynamics of the Slufter is comparable to that of primary tidal inlets, but there are pronounced differences. The most prominent difference with the nearby located primary inlets of the Wadden Sea is the hypsometric curve of the Slufter. At high water spring tide, almost 100% of the basin area of the primary tidal inlets in the Wadden Sea are covered (Maas, 1997). Only a relatively small salt marsh area is still dry. An increase of the high water level by a storm surge results in an increase of the tidal prism of the order of the basin area times the surge height. As shown in this paper the basin area of the Slufter is a strong function of the water level, also above the mean high water level at spring tide. Furthermore, the cross-sectional area of the inlet channel is also highly dependent on the water level. When applying the empirical relationships often the tidal prism at spring tide is taken. Using the results described in the previous section, this results in a predicted equilibrium cross-sectional area of 36 m^2 according to the O'brien relationship (O'brien, 1969) and 32 m^2 when data of the Dutch Wadden Sea is used (Stive & Rakhorst, 2008). In reality the cross-sectional area with respect to mean sea level is 18 m^2. The equilibrium relationships overpredict the real cross-sectional area by almost a factor 2.

Our results show that largest morphological changes occurred during the storm. One could therefore also argue that the tidal prism during the storm is determining the cross-sectional of the inlet. During the storm the mean water level was 0.8 metre and the cross-sectional area at this level is 48 m^2. The predicted equilibrium cross-sectional area is about 100 m^2. The cross-sectional area increased during the storm, but the duration of the storm was too short to deepen and widen the channel sufficiently. These results show that the present existing tidal prism cross-sectional area relationships are not performing very well for the Slufter. Furthermore, the predicted equilibrium cross-sectional area for storm conditions are much larger than for fair weather conditions. However, it is promising that for both types of conditions the equilibrium relationships overpredict the cross-sectional area by approximately a factor

https://doi.org/10.1017/S0016774600000470 Published online by Cambridge University Press

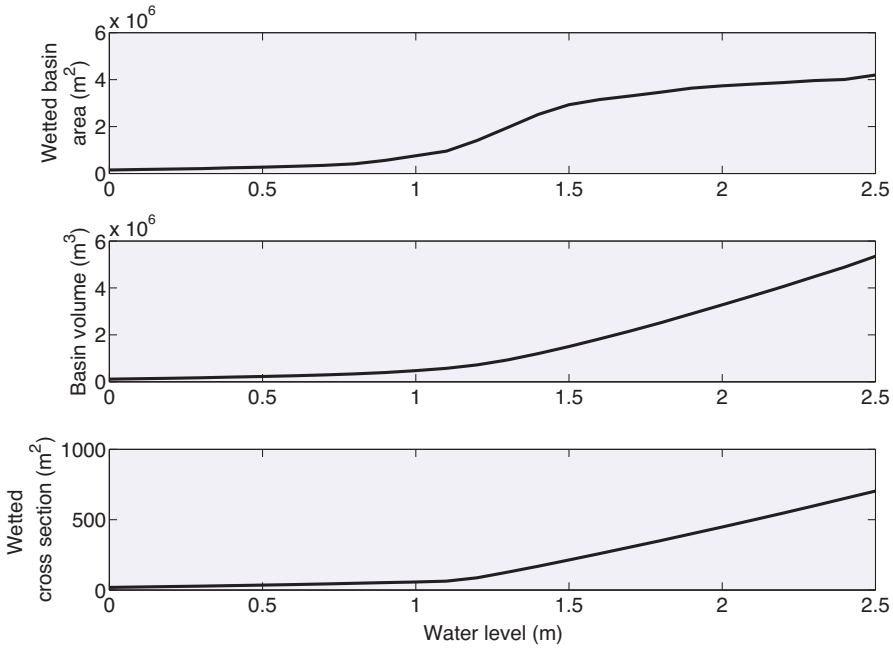

Fig. 16. Hypsometry of slufter as a function of water level.

two. This suggests that also for the Slufter a linear relationship exists.

The frequent relocation of the channel by man may also influences the dynamics. When the channel migrates to the south (or to the north before 1980) the channel length increases. Assuming that the typical water depth does not increase, this implies that the tidal prism increases. An increase of the length of the channel by 300 m results in an increase of the tidal prism of at least 10%. If channel relocation would not occur the channel would probably increase its length even further and maybe start eroding the dunes. However, the present opening between the dunes at the north and south side is not natural. We do therefore not know what the natural distance between the dunes would be. When the channel keeps increasing its length, at some point a new channel may be formed during a storm which has a shorter route to the sea. This also happens in many wave-dominated systems (Nghiem, 2009).

Another difference with primary tidal inlets is caused by the shallowness of the main channel of the Slufter, thereby causing a truncation of the tide with respect to the signal at sea (Lincoln & Fitzgerald, 1988). As a result, the ebb period is relatively long compared to the flood period. This would suggest an import of bed-load material (Friedrichs & Aubrey, 1988), but visual observations of the migration direction of the sand dunes suggest an export of bed-load material during calm weather (results not shown).

Due to the small water depths the dominant balance in the momentum equations is between friction and the pressure gradient. Hence, water levels are nonuniform within this small system. This contrasts the tidal dynamics within short primary tidal inlets (short with respect to the frictionless tidal wave length), which are well described by the pumping mode, implying uniform water levels in the backbarrier basin.

The dynamics of secondary tidal inlets compared to salt marshes.

The infrequent flooding of large parts of the Slufter is also common to washover areas and salt marshes. Large parts of the Slufter are only flooded at critical water levels above the mean spring tide high water level. These critical levels are determined by the height of the salt marsh areas and the height of the beach plain. This only occurs during storms and the salt marsh is flooded irregularly. Flow velocities in salt marsh channels often show two distinct peaks: one just after flooding of the salt marsh, and one during ebb at a water level well below the critical one (French & Stoddart, 1992; Fagherazzi et al., 2008). In the Slufter though, the peak flood flow is relatively weak and is equally strong during calm weather as during storm conditions. The largest flood flow measured occurred at a water level of +0.6 m (Julian day 274.2), which was not concurrent with a flooding event at that moment. In the Slufter the peak at the ebb phase is very pronounced, and it occurs when water levels in the main entrance channel are more than 0.5 m below the critical level of 1 m. The reason why the strong peak in flood flow is not observed is probably caused by the presence of the beach plain that is also flooded at a critical level of 1 m. Around the critical water level, the cross-sectional area of the main entrance increases faster than the basin area. Therefore, weaker flow velocities are needed. However, all the water is leaving the Slufter basin at a level below the critical. Hence, all the water is forced through a very small cross-section, resulting in the large flow velocities at ebb.

https://doi.org/10.1017/S0016774600000470 Published online by Cambridge University Press

The dynamics of secondary tidal inlets compared to washover areas

The processes that occur at the supratidal beach plain when it is flooded are equivalent to inundation overwash (Donnelly et al., 2006). The important parameters for inundation overwash are the surge level and the hydraulic gradient across the beach plain. They are determined by the astronomical tide, meteorological tide (wind set-up and inverse barometer effect) and wave set-up. During flood, when the critical level of the beach plain is exceeded, there is continuous inflow of water. Typical flow velocities are 0.5 to 0.8 m/s. In contrast to what is commonly observed in washover areas, in the Slufter the water does return to the sea again. This happens via the main channel. Averaged over a tidal cycle there is import of water and sediment via the beach plain, and export via the main channel. We were not able to quantify the amount of sediment import via the beach plain and export via the main channel, but we expect this balance to be crucial for the long term morphological evolution of the system.

The Slufter is a storm-dominated tidal inlet.

The maximum water level during the tidal cycle is the crucial parameter for the hydro- and morphodynamics of the Slufter. The Slufter rapidly evolves during short storm periods, while it evolves slowly or not at all during long periods with calm weather. Because of the crucial role of the storm surge level we consider this inlet to be a storm-dominated tidal inlet. This has strong implications for our thinking on the long-term morphodynamic evolution of secondary tidal inlets. Instead of trying to understand the dynamics of the Slufter during average conditions, one should try to understand the dynamics during average flooding conditions. The maximum water level reached during a tidal cycle and the height of the beach plain and salt marsh area are then the key parameters.

Conclusions

In this paper we studied the evolution of the Slufter on Texel on the long and on the short term. The results have shown that the seaward end of the Slufter channel is highly dynamic, while the landward part is characterised by a more gradual evolution. Since 1975 this landward part shows a southward migration and increase in curvature. Therefore the total length of the main channel has increased. Based on aerial photographs we conclude that in the 1970's the seaward end of the channel was migrating to the south. Since the 1980's this trend has reversed and the channel is migrating to the north. Based on yearly measured coastal profiles close to the Slufter inlet we showed that since 1963 there has been strong erosion of the mouth area. The vertical level of the beach plain has decreased and photographs suggest that the channel has deepened. Though, since 1979 the eroding trend is counteracted by regular beach nourishments and by the construction of the Eyerland dam in 1995.

Our results of the field campaign shed new light on the physical processes that drive the morphological evolution of secondary tidal inlets in general and the Slufter in particular. As a result of several flooding events during a storm period we have observed northward channel migration of 10 m, while the morphodynamic evolution during calm weather periods was very small. This strong evolution during a storm was driven by the flooding of the beach plain at the mouth area and the salt marsh areas in the backbarrier basin. This resulted in highly nonuniform flow patterns in the inlet. Averaged over a tidal cycle, there was import of water over the beach plain and export via the channel. During ebb flow velocities in the channel reached 2 m/s. The net channel migration was driven by erosion of the bed and channel banks by the ebb flows, whereas sedimentation occurred during flood at the south side of the channel by the sustained northward directed flow and sediment transport over the beach plain into the main channel.

Our results demonstrate that maximum water levels reached during storm periods are a key parameter to understand the morphological evolution of the system. The short-term and long-term evolution of the Slufter is driven by storms and it can be called a storm-dominated tidal inlet system.

Acknowledgements

We want to thank Ralf Klein Breteler, Wiebe Kramer and Stijn van Puijvelde or their help during their MSc research. This research would have been impossible without our technical staff: Marcel van Maarsseveen, Henk Markies, Chris Roosendaal and Bas van Dam.

References

Blanton, J.O., Linn G. & Elson, S.A., 2002. Tidal current asymmetry in shallow estuaries and tidal creeks. Continental Shelf Research, 22, 1731-1743.

Boon, J.D. & Byrne, R.J., 1981. On basin hypsometry and the morphodynamic response of coastal inlet systems. Marine Geology 40: 27-48.

Bruun, P. & Gerritsen, F., 1960. Stability of coastal inlets. North Holland, Amsterdam, 140 pp.

Bowman, D., 1993. Morphodynamics of the stagnating Zwin inlet, the Netherlands. Sedimentary Geology 84: 219-239.

Cooper, J.A.G., 2001. Geomorphological variability among microtidal estuaries from the wave-dominated South African coast. Geomorphology 40: 99-122.

Davis, R.A. & Hayes, M.O., 1984. What is a wave-dominated coast? Marine Geology 60: 313-329.

Donnelly, C., Kraus, N. & M. Larson, M., 2006. State of knowledge on measurement and modelling of coastal overwash. Journal of coastal research 22 (4): 965-991.

Ehlers, J., 1988. The morphodynamics of the Wadden Sea. Balkema (Rotterdam), 397 pp.

Eysink, W.D., 1990. Morphologic response of tidal basins to changes. Proceedings. 22nd International Conference on Coastal Engineering, ASCE, July, Delft, the Netherlands: 1948-1961.

Fagherazzi, S., Hannion, M. & D'Odorico, P., 2008. Geomorphic structure of tidal hydrodynamics in salt marsh creeks. Water resources research 44, W02419: doi:10.129/2007WR006289.

FitzGerald, D.M., 1996. Geomorphic variability and morphologic and sedimentologic controls on tidal inlets. Journal of Coastal Research 23: 47-71.

French, J.R. & Stoddard, J.R., 1992. Hydrodynamics of salt marsh creek systems; Implications of marsh morphological development and material exchange. Earth surface processes and landforms 17: 235-252.

Friedrichs, C.T. & Aubrey, D.G., 1988. Non-linear tidal distortion in shallow well-mixed estuaries: a synthesis. Estuarine Coastal and Shelf Science 27: 521-545.

Hubbard, D.K., Oertel, G.F. & Nummedal, D., 1979. The role of waves and tidal currents in the development of tidal-inlet sedimentological structures and sand body geometry: Examples from North Carolina, South Carolina and Georgia. Journal of Sedimentary Petrology 49: 1073-1093.

Lincoln, J.M. & FitzGerald, D.M., 1988. Tidal distortions and flood dominance at five small tidal inlets in southern Maine. Marine Geology 82: 133-148.

Maas, L.R.M., 1997. On the nonlinear Helmholtz response of almost-enclosed tidal basins with sloping bottoms. Journal of fluid mechanics 349: 361-380.

Meerkerk, A.L., Arens, S.M., Van Lammeren, R.J.A. & Stuiver, H.J., 2007. Sand transport dynamics after a foredune breach: A case study from Schoorl, the Netherlands. Geomorphology 86: 52-60.

Nghiem, T.L., 2009. Hydrodynamics and morphodynamics of a seasonally forced tidal inlet system. PhD-thesis Delft University of Technology.

O'Brien, M.P., 1969. Equilibrium flow areas of inlets on sandy coasts. J. Waterway Port Coast Ocean Eng 95: 43-52.

Oost, A.P. & De Boer, P.L., 1994. Sedimentology and development of barrier islands, ebb-tidal deltas, inlets and backbarrier areas of the Dutch Wadden Sea. Senckenbergiana Maritima, 24: 66-115.

Powell, M.A., Thieke, R.J. & Mehta, A.J., 2006. Morphodynamic relationships for ebb and flood delta volumes at Florida's tidal entrances. Ocean Dynamics 56: 295-307.

Sha, L.P., 1989. Variation in ebb-delta morphologies along the west and east Frisian islands, the Netherlands and Germany. Marine Geology, 89: 11-28.

Stive, M.J.F. & Rakhorst, R.D., 2008. Review of empirical relationships between inlet cross-section and tidal prism. Journal of Water Resources and Environmental Engineering, no 23, November 2008.

De Swart, H.E. & Zimmerman, J.T.F., 2009. Morhodynamics of tidal inlet systems. Annual Review of Fluid Mechanics. doi: 10.1146/annurev.fluid.010908.165159.

Van Bohemen, H.D., 1996. Environmentally friendly coasts: dune breaches and tidal inlets in the foredunes. Environmental engineering and coastal management. A case study from the Netherlands. Landscape and Urban Planning 34: 197-2313.

Van der Vegt, M, Hoekstra, P. & Van Puijvelde, S.P., 2009. Channel migration in a small tidal inlet. *In:* Vionnet, C.A., Garcia, M.H., Latrubesse, E.M. & Perillo, G.M.E. (eds): Proceedings of the 6th RCEM conference 2009, Santa Fe, Argentina. Balkema: 169-176.

Van der Vegt, M., Schuttelaars, H.M. & De Swart, H.E., 2007. Modeling the formation of undulations of the coastline: The role of tides. Continental Shelf Research, 27: 2014-2031.

Walton, T.L. & Adams, W.D., 1976. Capacity of outer bars to store sand. *In:* proceedings of the 15th ICCE. ASCE, New York: 1919-1938.

https://doi.org/10.1017/S0016774600000470 Published online by Cambridge University Press